

# Effects of Diluents on the Behavior of the Diluted Combustion Regime

Yuying LIU<sup>1</sup>, Jean-Michel MOST<sup>\*,2</sup>

<sup>1</sup>School of Jet Propulsion, Beijing University of Aeronautics and Astronautics

<sup>2</sup>Laboratoire de Combustion et de Détonique (LCD), CNRS, ENSMA, France, F-86961 Futuroscope Cedex

## Abstract

The diluted combustion regime is studied with a non-premixed counter flow flame, in which methane and air are both preheated and diluted by N<sub>2</sub> or N<sub>2</sub>/CO<sub>2</sub>. The flame stability diagram is presented for various diluents composition via changing the concentration of N<sub>2</sub>/CO<sub>2</sub> ratio in diluents. Hydroxyl radical Planar Laser Induced Fluorescence (OH-PLIF) technique is used to analyze the effects of diluents, preheat temperature and fuel or oxygen concentration on the reaction zone characteristics, such as OH radical intensity distribution and reaction zone thickness, and an estimated flame temperature is introduced simultaneously. The results show that much CO<sub>2</sub> in the diluents decrease the flame stability, especially for low oxygen concentration conditions, but preheating of reactants broadens the flammability domain. The preheat temperature shows more prominent effects on the flame thickness than reactant concentration under the flame condition examined. The addition of CO<sub>2</sub> into the reactants lowers the OH intensity, flame temperature and the reaction zone thickness more efficiently than pure N<sub>2</sub> dilution mainly because of its higher heat capacity.

## Introduction

With the rapid increase of global demand for energy, conventional combustion technology of fossil fuel faces dual challenge in energy-saving and environmental protection. Preheating of combustible mixture by recycled heat from exhaust gases has been considered as an effective method not only for combustion of low calorific fuels but also for fuel conservation and low-NO<sub>x</sub> emission purpose since last century [1], in which combustion reactants are preheated and diluted at the same time. Extensive studies on diluted combustion with highly preheated temperature reactants have been conducted for the past decades with various nominal definition, such as “High Temperature Air Combustion (HiTAC)”[2], “flameless combustion or FLOX® (Flameless Oxidation)”[3], “mild combustion (Moderate or Intense Low-oxygen Dilution Combustion)”[4] and “Highly Preheated Air Combustion (HPAC)” [1,5], in which the combination of the exhaust gas recirculation and high temperature air are well utilized. And the air temperature is high enough to achieve the auto ignition temperature of combustion mixture, which is higher than 800°C (depending on fuel, oxygen concentration and combustion device) in generally [5]. In contrast, as an important part of this low-NO<sub>x</sub> diluted combustion technology concept, few studies on the diluted combustion regime with reactants under the auto ignition temperature, which is named as preheated air combustion (PAC) by M. Katsuki [1], can be found.

Among those studies on diluted combustion, the flame characteristics, such as flame stability, NO<sub>x</sub> emission, flame temperature uniformity, flame shape or flame length, etc, are studied under various diluted combustion conditions. For example, K. Maruta (2000) [6] experimentally has studied the flammability limit

and reaction zone properties of N<sub>2</sub> diluted counter flow flame with air temperature 300K~800K, and founded that extinction limit is widened with air temperature increase and the structure of flame is similar to that of conventional combustion; K. Murata (2007) [7] has examined the extinction characteristics of CO<sub>2</sub> diluted methane-air counter flow non-premixed flames at elevated pressures up to 0.7 MPa experimentally and computationally under the background of oxygen combustion for gas turbine combustors, and conventional C-shape extinction curves are observed at ambient pressure; T. Ishiguro [8] has showed that flames with highly preheated air (1000 °C) diluted by nitrogen is much more homogeneous and stable than the flames of room-temperature air, and the flame length with 10% volume fraction of oxygen in air is greater than that of 20%; K. Gupta et al [9] have examined the exhaust gas diluted propane flame with air temperature from 900°C to 1100°C and oxygen concentration from 21% to 2% in a regenerator burner, and concluded that flame volume and flame length increases with the increasing of air temperature and decreasing of oxygen concentration; S. Lille et al [10] have experimentally studied a flue gas diluted cross-flow flame of highly preheated (up to 900±°C) oxidizer, and the oxygen concentration is found to have a substantial effect on flame size, liftoff distance, moreover, a lower oxygen concentration increases the flame size and the liftoff distance, and temperature has the opposite effect of decreasing the flame size but not in the same proportions as an increase in oxygen concentration; J. Yuan [11] numerically investigated the effects of air dilution on highly preheated air (1223K) combustion in a regenerative furnace using nitrogen, carbon dioxide, helium, argon, and flue gas as diluents, and concluded that heat capacity of the diluted air plays an important

---

\*Corresponding author: [jean-michel.most@lcd.ensma.fr](mailto:jean-michel.most@lcd.ensma.fr)  
European Combustion Meeting 2009

role in the effect of diluents on flame temperature, the temperature uniformity, and the NO<sub>x</sub> emission; G. J. RØrtveit [12] has investigated the NO<sub>x</sub> emission of fuel diluted hydrogen counter flow flame using different diluents such as nitrogen, carbon dioxide and helium, and the influences of various diluents are discussed in terms of differences in heat capacities, thermal-radiative properties, and effects on chemical reactions. Consequently, the effects of preheat temperature, fuel or oxygen concentration and diluent composition, play an important role in the diluted combustion.

The objective of this paper will be to enhance the knowledge on these effects of diluents composition, moderate preheat temperature and reactants concentration on the behavior of a diluted combustion. A mixture of nitrogen and carbon dioxide were chosen as diluents in this experiment for their relevance to recirculation of burned hydrocarbon flue gases. The oxidizer is air in the present work. The flame stability and the reaction zone characteristics are experimentally studied on the basis of a non-premixed methane-air counter flow burner flame with preheat temperature from ambient to 750°C.

## 2 Experiment Setup

### 2.1 Counter flow burner system

The counter flow burner used in this experiment is illustrated schematically in Fig.1. Fuel stream (top) and oxidizer stream (bottom) issues from two identical vertically opposed nozzles. The separation distance (H) between the nozzles of the counter flow burner can be changed but equals to 35mm in this experiment. An annular concentric co-flow of nitrogen is established to provide a curtain in order to prevent the reaction of fuel with surrounding air. Methane and air is used as fuel and oxidizer respectively, and both fuel and oxidizer is diluted by nitrogen and carbon dioxide simultaneously. The flow on each side is electrically heated up, and passes through a perforated plate (approximately 50% blockage, holes diameter 3 mm, holes spacing 3.7mm, located at 0.250m upstream of the nozzle exits) to break residual turbulence; a tranquilization pipe follows it. The internal injection diameter D is 35 mm. A computer-controlled gas mixing system allows an accurate control of reactant concentration and preheat temperature and flow velocity (or mixture mass flow rate). The non-premixed CH<sub>4</sub>/Air flame is experimentally established with reactants diluted in nitrogen and carbon dioxide. The flow rates injected on both sides are kept constant for a cold stream velocity of  $u_c = 0.5m/s$ , corresponding to a constant volume flow rate of  $Q_c \approx 4.82 \times 10^{-4} m^3/s$ . As the two reactant flows are heated up, their effective velocities  $u_h$  at the exhaust change. The average exhaust velocity after preheating follows the law:

$$u_h = (u_c / T_c) \cdot T_{pr} \quad (1)$$

where  $u_h$  is the exhaust velocity of hot reactants,  $u_c$  is the inlet cold flow velocity,  $T_c$  is the temperature of reactant inlet ( $T_c \approx 298K$ ), and  $T_{pr}$  is the preheat temperature (298~1023K). The volume fraction of

methane  $X_{CH_4}$  in the fuel stream varies from 6 to 30%, and the oxygen volume fraction  $X_{O_2}$  in the oxidizer stream ranged from 10 to 21%, and is referred as *reactant concentrations*, which can represent the dilution level simultaneously. The volume fraction of carbon dioxide  $X_{CO_2}$  varies from 0~20% and keeps identical for fuel and oxidizer flow in this experiment. For the case  $X_{CO_2}$  equals to zero, the diluents is pure nitrogen; for the case  $X_{CO_2}$  not equals to zero, the remaining part of diluents is nitrogen. And it follows:

$$X_{CH_4} = 1 - X_{CO_2} - X_{N_{2f}} \quad (2a)$$

$$X_{O_2} = 1 - X_{CO_2} - X_{N_{2o}} \quad (2b)$$

where  $X_{N_{2f}}$  and  $X_{N_{2o}}$  are the volume fraction of nitrogen in the fuel and oxidizer flow respectively.

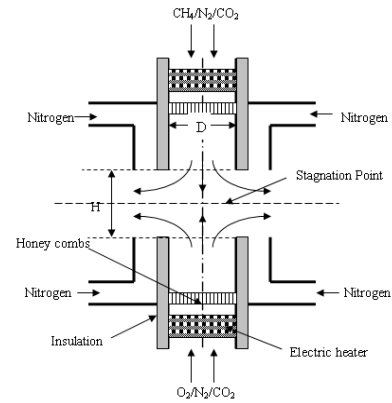


Fig.1 Schematic map of the experimental counter flow burner

### 2.2 OH-PLIF detection system

Visualization of the reaction zone by PLIF allows localizing combustion reaction zone. Transient locations of the reaction zones can be identified by radical distributions such as OH or CH. To excite the fluorescence of OH radical, a second harmonic of a Q-switched infra-red pulsed Nd: YAG laser at 532nm is used to pump a tunable dye laser (ND6000, Continuum). The frequency doubled beam is tuned at 282.910nm to excite the Q1(6) transition of the A-X(1-0) band of OH radical in this experiment. The beam is spread into a vertical sheet with the help of a series of sheet-forming optics, and the sheet of light traverse the centerline of counter-flow burners. An ICCD camera (PI-MAX2, Princeton Instruments) equipped with a UV lens (Cerro 2017 UV-VIS-NIR, 45mm, f/1.8) is used to detect the two-dimensional fluorescence from the excited molecule OH. A combination of Scott glass UG11 and WG305 filters is placed in front of the camera to avoid detection of flame luminosity and spurious light scattering. Images are collected in the direction orthogonal to the laser sheet, providing black-and-white measurement on a 581\*591 pixels matrix. The spatial resolution was 133µm per pixel. To provide a sound basis for analysis, 100 single-shot OH distributions are taken for each experimental flame condition.

### 3 Results and Discussion

#### 3.1 Flame stability map

Flame stability map is determined by extinction test firstly in this study. The extinction tests are performed by gradually decreasing the volume fraction of methane in fuel stream  $X_{CH_4}$  until flame extinction is achieved under constant volume fraction of oxygen  $X_{O_2}$  in oxidizer stream after stable flame is established between the two counter flow jets: then  $X_{CH_4}$  is recorded. For various given point ( $u_c=0.5m/s$ ,  $T_{pr}=298\sim 1023K$ ,  $X_{O_2}<21\%$ ), the experiment is repeated several times in order to achieve sufficient precision on the determined limit. The flow field strain rate  $S$  based on the flow exit velocity  $u_h$  can be defined as [12]:

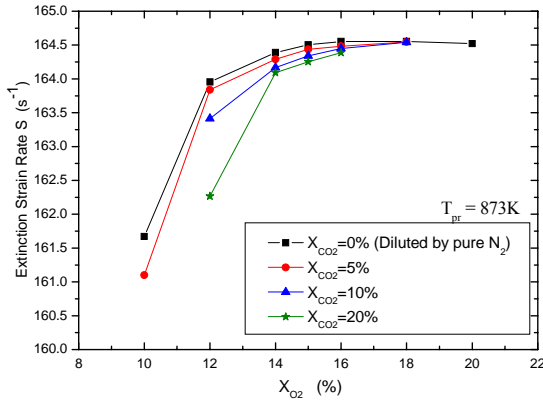
$$S = (2u_h / H)(1 + \sqrt{\rho_F / \rho_O}) \quad (3)$$

in which

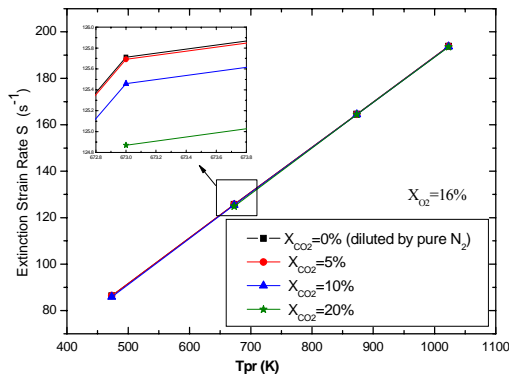
$$\rho_F = X_{CH_4} \cdot \rho_{CH_4} + X_{CO_2} \cdot \rho_{CO_2} + X_{N_{2f}} \cdot \rho_{N_2} \quad (4a)$$

$$\rho_O = X_{O_2} \cdot \rho_{O_2} + X_{CO_2} \cdot \rho_{CO_2} + X_{N_{2o}} \cdot \rho_{N_2} \quad (4b)$$

where  $\rho$  is the density and varies with preheat temperature, but here  $T_{pr}$  is omitted for simplify. Subscript  $F$  and  $O$  represent fuel-stream and oxidizer-stream mixture respectively, and subscript  $CH_4$ ,  $O_2$ ,  $CO_2$ ,  $N_{2f}$  and  $N_{2o}$  represent the mixture components.



(a)



(b)

Fig.2 Flame stability map

Figure 2 presents the flame stability diagram using extinction strain rate  $S$  as the function of oxygen concentration  $X_{O_2}$  and preheat temperature  $T_{pr}$ . Figure 2(a) shows that extinction strain rate decreased with the oxygen concentration  $X_{O_2}$  decrease both for nitrogen dilution ( $X_{CO_2} = 0$ ) and nitrogen plus carbon dioxide dilution, which means that much oxidizer dilution makes flame less stable whatever diluent composition is. It also can be found that, extinction strain rate  $S$  decreased with the  $CO_2$  content increasing under certain oxygen concentration and preheat temperature condition. Simultaneously, the effect of  $CO_2$  concentration on the flame stability is noticeably increased as the oxygen concentration decreased. In other words, compare with  $N_2$ , much  $CO_2$  in the diluents reduce the flame stability, especially for low oxygen concentration condition. Figure 2(b) shows that the extinction strain rate  $S$  for a sustainable combustion increased with the increasing of preheat temperature  $T_{pr}$  for given oxygen concentration  $X_{O_2}$  and diluents composition ( $X_{CO_2}$  equals to constant). But it decreases with the increasing of carbon dioxide concentration  $X_{CO_2}$  under a given preheat condition, as reported in Figure 2(a). Obviously, preheating broadens the flammability domain of flame, and much  $CO_2$  in the diluents weaken the flame stability.

#### 3.2 OH intensity distribution

The OH intensity distribution represents approximately the concentration distribution of OH in the reaction zone. Average OH-PLIF image of the 100 frames is used to show the OH intensity distribution for each flame condition, and a region of interesting (ROI) is cut symmetrically from the raw OH-PLIF image along burner axis within the inlet injection diameter range during image processing. Fig.3 presented one typical OH intensity image of flame in ROI.

Considering the OH signal corresponds to the higher temperature region where the reaction takes place, an estimated flame temperature  $T_{ad}$  is introduced before presenting OH intensity distribution using the analysis solution according to Burck-Shuman's assumption for this counter flow diffusion flame as following [14]:

$$T_{ad} = T_{pr} + (Q \cdot Y_{F0} / C_p) \cdot z_{st} \quad (5)$$

where  $Q$  is the heat of reaction or the lower heat value of methane,  $Y_{F0}$  is the mass fraction of methane in the pure fuel stream,  $C_p$  is the specific heat of gas mixture, which is assumed to be constant and equals to that of nitrogen,  $z_{st}$  is the mixture fraction at stoichiometry (for counter flow laminar diffusion flame  $z_{st} = 1 / (\phi + 1)$ , where  $\phi = s \cdot (Y_{F0} / Y_{O0})$  is the equivalence ratio and  $Y_{O0}$  is the mass fraction of oxygen in the oxidizer stream). The stoichiometric mass oxidizer and fuel ratio  $s$  equals to 4 for the complete oxidation of methane. That is:

$$T_{ad} = T_{pr} + [Q / C_p / (4 / Y_{O0} + 1 / Y_{F0})] \quad (6)$$

This estimated flame temperature  $T_{ad}$  from eq.6 and the average OH peak intensity from PLIF image is listed in Table.1 for some typical cases simultaneously. Although  $T_{ad}$  is relatively higher than the real flame temperature because of constant nitrogen  $C_p$  is used in the calculations, the variation of it is well estimated for the diluted combustion.

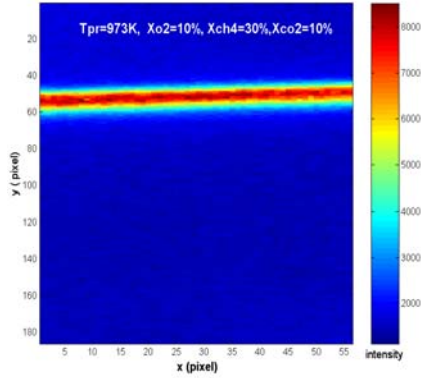


Fig.3 Typical OH intensity image from PLIF (ROI)

Table 1 OH peak intensity and estimated flame temperature for test cases

Cases		Oxidizer Stream Composition (%)			Fuel Stream Composition (%)			Estimated Flame Temperature (K)	Maximum OH intensity by PLIF
		O <sub>2</sub>	dilutents		CH <sub>4</sub>	dilutents			
			X <sub>CO2</sub>	X <sub>N2o</sub>		X <sub>N2r</sub>	X <sub>CO2</sub>		
I	T <sub>pr</sub> =973K	10	90	0	70	0	2095.3	11238	
			85	5	30	65	5	2063.9	9156.5
			80	10		60	10	2034.3	7566.6
II	T <sub>pr</sub> =973K	14	86	0	70	0	2462.2	13005	
			81	5	30	65	5	2420.5	11152
			76	10		60	10	2343.8	10267
III	T <sub>pr</sub> =973K	18	82	0	70	0	2792.8	13595	
			77	5	30	65	5	2741.8	12272
			72	10		60	10	2693.5	11204
IV	T <sub>pr</sub> =973K	18	82	0	82	0	2724.5	12319	
			77	5	18	77	5	2503.9	11889
			72	10		72	10	2462.2	10408
V	T <sub>pr</sub> =973K	18	82	0	92	0	2548.1	10389	
			77	5	8	87	5	2051	9501.7
			72	10		82	10	2021.7	7742.2
VI	T <sub>pr</sub> =673K	18	82	0	70	0	2492.8	9673.2	
			77	5	30	65	5	2441.8	8670.1
			72	10		60	10	2393.5	7880
VII	T <sub>pr</sub> =473K	18	82	0	70	0	2292.8	8121.7	
			77	5	30	65	5	2241.8	7024.2
			72	10		60	10	2193.5	5586.4

Fig.4 to Fig.6 present the effects of fuel or oxygen concentrations, preheat temperature  $T_{pr}$  and diluent compositions (marked by CO<sub>2</sub> concentration  $X_{CO2}$ ) on the OH intensity distribution of flame along the axis of burner, which is noted by  $y$  from up to down of Fig.3. *Firstly*, similar to Table 1, Fig.4 (case I & III) and Fig. 5 (case IV & V) shows that OH peak intensity decreases with the decreasing of oxygen concentration  $X_{O2}$  or fuel concentration  $X_{CH4}$  under constant preheat temperature. Fig. 6 (case III, VI & VII) shows that OH peak intensity increases with the increase of preheat temperature  $T_{pr}$  at certain reactant concentration. Those phenomena are similar to the observation of flame spontaneous luminosity from naked eyes. The increasing trend for peak OH concentration with the increase of preheat

temperature and reactant concentration is due to the increase in flame temperature and the availability of more oxygen atoms in the flames. Moreover, the OH profiles also become narrower with decrease of fuel or oxygen concentration and preheat temperature. *Secondly*, the location of OH peak shifted toward to the “lean” side of counter flow at constant preheat temperature, it shifts toward to oxidizer side with the decrease of oxygen concentration  $X_{O2}$  (Fig.4), and towards to fuel side with the decrease of fuel concentration  $X_{CH4}$  (Fig.5). It shifts towards to oxidizer side when preheat temperature increase (Fig.6). *Last but not the least*, from Table.1 and Fig.4 to Fig.6, it shows that at given fuel or oxygen concentration and preheat condition, the peak OH concentration and flame temperature decrease and OH profiles become narrower with the increasing of CO<sub>2</sub> content in diluents. Carbon dioxide dilution gives a lower OH signal and flame temperature than the nitrogen dilution ( $X_{CO2} = 0$ ) under all tested fuel and oxygen concentrations and preheat condition. It shows that CO<sub>2</sub> lowers the OH signal and flame temperature more efficiently than N<sub>2</sub> diluents. As inferred by J. Yuan & I. Naruse [4], CO<sub>2</sub> is more effective than N<sub>2</sub> on the aspect of temperature uniformity, the difference between N<sub>2</sub> and CO<sub>2</sub> in the heat capacity, represented by the product of the specific heat and density, can be an important factor resulting in the OH signal difference, which is related to the flame temperature. In details, for example, carbon dioxide and nitrogen have a specific heat of 1.235K/JKg·K and 1.170K/JKg·K, a density of 0.5438 Kg/m<sup>3</sup> and 0.3388 Kg/m<sup>3</sup> at 1000K respectively. The higher heat capacity corresponds to the lower flame temperature. This is also reasonable to explain the effects of CO<sub>2</sub> on the flame stability and agree well with the phenomena reported in the 3.1 section.

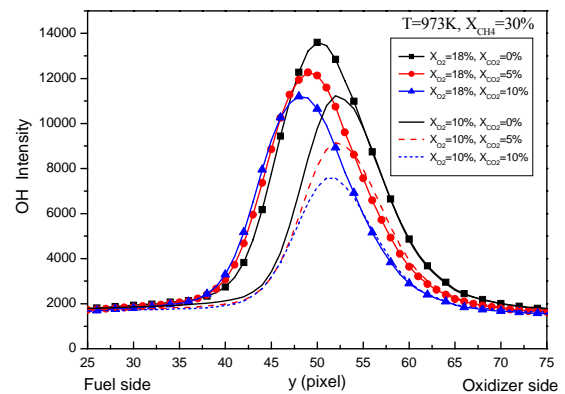


Fig.4 Effects of oxygen concentration ( $X_{O2}$ ) and diluents composition on OH intensity distribution

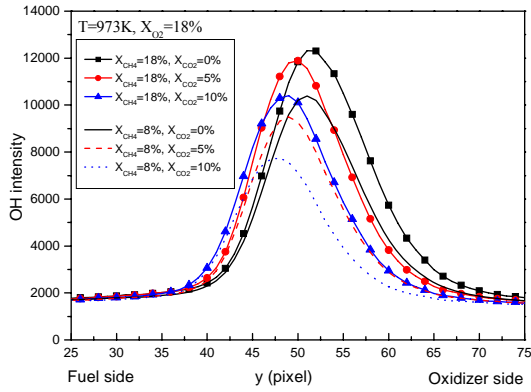


Fig.5 Effects of fuel concentration ( $X_{CH_4}$ ) and diluents composition on OH intensity distribution

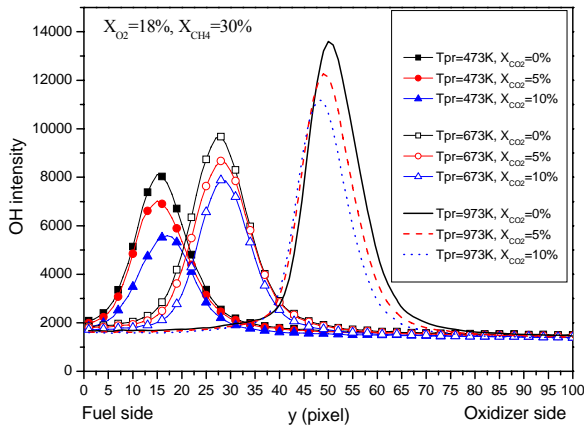


Fig.6 Effects of preheat temperature on OH intensity distribution

### 3.3 Reaction zone thickness from OH-PLIF

The thickness of OH radical zone got from OH-PLIF image, here named as reaction zone thickness, is studied for stable flame conditions to analyze the effects of reactant concentration ( $X_{O_2}$  and  $X_{CH_4}$ ), preheat temperature  $T_{pr}$  and diluent composition ( $X_{CO_2}$ ) further. An image-processing program based on threshold method is used to get the reaction zone thickness from 100 single-shots OH-PLIF images, and then an average reaction zone thickness  $\delta_{OH}$  of those 100 frames is determined for each flame condition. A normalized reaction zone thickness  $\delta_{OH}/H$  by the separation distance  $H$  between two nozzles is used in the following discussions.

Fig. 7 to Fig.9 shows that reaction zone thickness increases with the oxygen or fuel concentration and preheat temperature whatever diluents composition is, as their influence on the OH intensity distribution and flame luminosity from naked eyes. From the chemical reaction point of view, the chemical reaction rate decreases with dilution and increases with preheat. Therefore, in the diluted combustion systems where both dilution and preheat exist, the reaction rate is dominated by the two parameters together. From Fig. 7 and 8, it can be seen that flame thickness became thinner with the increase of dilution (decreasing of fuel and oxygen concentration) under constant preheat temperature. It implies that the increasing effect of

reaction rate due to preheat is more prominent than the decreasing effect of reaction rate due to dilution in the condition of examined. Preheat temperature is the main influential parameter of diluted combustion with preheated reactants in this experiment. However, from the work of T. Ishiguro et al [8], A. K .Gupta et al [9] and S. Lille et al. [10], lower oxygen concentration (higher dilution level) increases the flame size or flame length in condition of diluted combustion with highly preheated reactants, and oxygen concentration is considered the primary influential parameters in this kind of combustion regime. It shows that the controlling parameters of diluted combustion may be different under various levels of preheated reactants. When preheat temperature is high enough to start flameless combustion as in [8-10], the decrease effect of reaction rate due to dilution is larger than the increase effect of reaction rate due to temperature increasing, and reactants concentration (or dilution level) became the main factor of diluted combustion with highly preheated reactants. Fig.9 shows that reaction zone thickness increases with the increase of preheat temperature under constant reactant concentration, this is agree well with the results of literature [8-10] fore mentioned, in which reactants is highly preheated and diffusion of reactants increased. Under highly preheated and diluted reactant condition as reported in the literature, because of the strong diffusion of reactants and reaction rate decreasing, the flame takes a dispersed form, or even, looks like flameless.

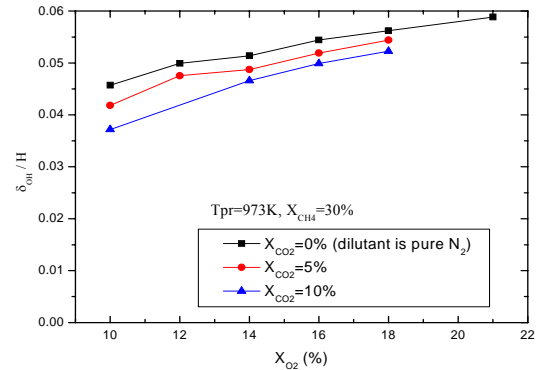


Fig. 7 Effects of oxygen concentration and diluents composition on reaction zone thickness

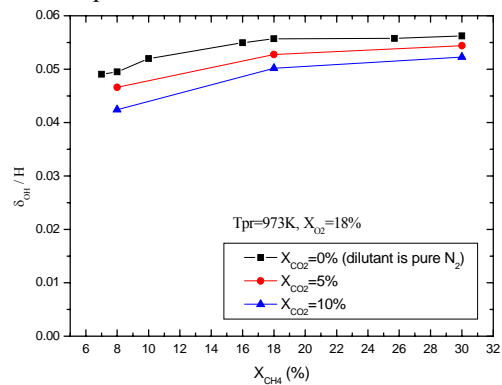


Fig. 8 Effects of fuel concentration and diluents composition on reaction zone thickness

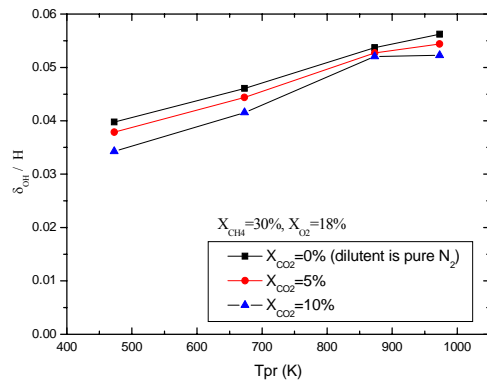


Fig. 9 Effects of preheat temperature and diluents composition on reaction zone thickness

Moreover, Fig. 7 to Fig.9 show that reaction zone thickness decreases with the increase of carbon dioxide concentration in diluents at same reactant concentration and preheat temperature. Nitrogen dilution ( $X_{CO_2} = 0$ ) demonstrates thicker reaction zone compare with nitrogen plus carbon dioxide dilution. This observation enforces the conclusions reached from the OH intensity distribution and estimated flame temperature in section 3.2 and highlights the fact that  $CO_2$  is more effective than  $N_2$  to lower the OH intensity, flame temperature and the temperature uniformity, which is helpful for the abating of  $NO_x$  emission. This is essential because  $CO_2$  has higher heat capacity than  $N_2$ . But, according to the analysis of A. Cavaliere [4] for a WSR mild combustion model, the  $CO_2$  content in diluents can change the behavior of diluted combustion not only because it can affect the heat capacity of the system but also because it can contribute in the chemical reaction.

#### 4. Conclusions

This paper reports the effects of fuel and air dilution with  $N_2$  or  $N_2+CO_2$  on the behavior of diluted combustion under various preheat temperature operating condition in a counter flow burner. The flame stability map and the reaction zone structure are investigated under various reactant concentrations (or dilution levels), preheat temperature, and diluent composition. The OH-PLIF method is used to analyze the intensity distribution and reaction zone thickness in the diluted combustion in details. The conclusion can be presented as following:

- (1) Preheating of reactants broadens the flammability domain of diluted combustion flame. Oxidizer dilution makes flame less stable whatever diluents composition is. Compare with  $N_2$ , much  $CO_2$  in the diluents decrease the flame stability, especially for low oxygen concentration conditions;
- (2) The OH maximum intensity shifts towards to the “lean” side of counter flow at constant preheat temperature, and it shifts toward to fuel side with the increase of dilution ratio of fuel stream and towards to the oxidizer side with the increase of oxidizer stream respectively;
- (3) OH intensity, flame temperature and the reaction zone thickness increase with the reactant

concentration at constant preheat temperature and increase with preheat temperature at fixed dilution levels. The effects of preheat temperature on the reaction zone thickness is more important than that of reactant concentration under the flame condition examined; it is the most important parameter of diluted combustion in the studied domain;

- (4) The addition of  $CO_2$  into the reactants lowers the OH intensity, flame temperature, the reaction zone thickness more efficiently than pure  $N_2$  dilution mainly because of its higher heat capacity.

#### Acknowledgements

The support and funding of CNRS “ACI-Energie” Programme, French minister of Research, the Region Poitou-Charentes of France and National Natural Science Foundation of China (No: 50606004) are gratefully acknowledged for this work.

#### References

- [1]. M. Katsuki, T. Hasegawa, Proc. Combust. Inst. 27 (1998) 3135-3146.
- [2]. H. Tsuji, A. K. Gupta, T. Hasegawa, et al., High Temperature Air Combustion (From Energy Conservation to Pollution Reduction), CRC Press LLC, USA, 2003.
- [3]. J. A. Wüning, J. G. Wüning, Prog. Energy Combust. Sci. 23 (1997) 81-94.
- [4]. A. Cavaliere, M. de Joannon, Prog. Energy Combust. Sci. 30 (2004) 329-366.
- [5]. T. Plessing, N. Peters, J. G. Wüning, Proc. Combust. Inst. 27 (1998) 3197-3204.
- [6]. K. Maruta, K. Muso, K. Takeda, et al., Proc. Combust. Inst. 28 (2000) 2117-2123.
- [7]. K. Maruta, K. Abe, S. Hasegawa, et al., Proc. Combust. Inst. 31 (2007) 1223-1230
- [8]. T. Ishiguro, S. Tsuge, T. Furuhashi, et al., Proc. Combust. Inst. 27 (1998) 3205-3213.
- [9]. A. K. Gupta, AIAA 99-0725, 37th AIAA Aerospace Sciences Meeting and Exhibit, 1999.
- [10]. S. Lille, T. Dobski, W. Blasiak, Journal of Propulsion and Power, 16(2000) 595-600.
- [11]. J. Yuan, I. Naruse, Energy & Fuels, 13(1999) 99-104
- [12]. G. J. Rørtveit, J. E. Hustad, S.C. Li and A. Williams, Combustion and Flame, 130 (2002) 48-61
- [13]. P. Bauer, Etude expérimentale d’un régime de combustion diluée dans une configuration à contre-courant, PhD thesis, l’Université de POITIERS, Poitiers, France, 2006
- [14]. T. Poinso and D. Veynante, Theoretical Numerical Combustion, Second Edition, Edwards, USA, 2005